J. Min. Metall. Sect. B-Metall. 60 (2) (2024) 205 - 214

Journal of Mining and Metallurgy, Section B: Metallurgy

PYROMETALLURGICAL TREATMENT OF JAROSITE RESIDUE WITH A MIXTURE OF CaO, SiO_2, AND CaSi

C. Jiménez-Lugos [a], M. Flores-Favela [b], A. Romero-Serrano [a,*], A. Hernández-Ramírez [a], J. López-Rodríguez [a], A. Cruz-Ramírez [a], E. Colin-García [a]

[a] Instituto Politécnico Nacional, ESIQIE, Metallurgy and Materials, Ciudad de México, Mexico
[b] Servicios Administrativos Peñoles S.A de C.V.Prol. Comonfort Sur 2050, Col. L. Echeverría, Torreon, C.P. Coahuila, Mexico

(Received 19 December 2023; Accepted 17 September 2024)

Abstract

During the electrolytic production of zinc, the iron in solutions is mainly controlled by the precipitation of jarosite. This precipitate also contains valuable metals (Zn, Pb, Cu, Ag) and toxic elements (Hg, Cd, As). This study deals with the pyrometallurgical treatment of jarosite waste in order to recover the metal values and convert the waste into environmentally acceptable slag. Initially, the sample was heated to 100 °C to remove moisture, and then roasted at 700 °C to release some OH^- and sulfate groups by thermal decomposition. The analysis of the SiO_2-CaO-Fe_2O_3 ternary phase diagram showed that a flux containing 48% CaO and 52% SiO_2 can be used to melt the roasted jarosite at 1400 °C. Subsequently, tests were carried out with the reducing agent (CaSi), resulting in a mixture of slag and two metallic phases, one of which is an Fe-Si alloy and the other a Pb-rich phase containing the valuable metal Ag. Both the metallic and slag phases were characterised by chemical analysis, SEM-EDS and XRD. Additionally, the raw jarosite residue and the final slag were leached with an aqueous acetic acid solution to estimate their chemical stability. The obtained results show that the slag produced after the reduction of jarosite residue meets the environmental specifications and could be used as raw material in other industries.

Keywords: *Jarosite; Thermal processing; Metal recovery*

1. Introduction

Iron is a primary impurity in zinc production, and the jarosite process is widely employed to remove it due to its simplicity and cost-effectiveness [1]. In this process, the jarosite, $XFe_3(OH)_6(SO_4)_2$ where X = Na, K, H_3O, NH_4, is precipitated by the addition of sodium, potassium, or ammonium sulfate [2]. Zinc hydrometallurgy constitutes over 85% of the world's zinc weight, generating millions of tons of jarosite residue annually. The need for storage results in significant land occupation [3]. Moreover, jarosite residues, containing metals such as lead, zinc, silver, and arsenic, are deemed hazardous waste contributing to environmental issues and causing ecological problems [4, 5].

It is estimated that jarosite residue production is approximately 0.5 tons for every ton of zinc produced. Therefore, the jarosite produced from the zinc hydrometallurgical process needs urgent handling [6]. Specifically, the jarosite residue has a high content of heavy metal ions and poor stability. Consequently, jarosite is classified as hazardous industrial solid waste [7, 8]. Prolonged piling of jarosite residues can cause serious damage to the environment, soil, water sources, and human health. Therefore, it is imperative to treat and use jarosite residues.

Several efforts have been made to treat jarosite residues and recover valuable metals from waste. Various methods have been adopted for metal recovery. One approach involves the addition of coke powder to the waste, then heating the mixture to 1200 °C to volatilise zinc and lead, recovering these metals. Although efficient, this process has high energy consumption and leads to air pollution [9, 10]. In an alternative method, jarosite residues are directly reduced with coal sludge. This achieves good volatilisation of Zn and Pb, along with high iron recovery; sulfur in the residues, however, is a contaminant for the obtained iron [11]. Jiang et al. [12] proposed roasting jarosite residue to break down stable forms of metals and subsequently leaching them to recover the valuable metals. Using an NH_4Cl solution as a leaching agent allows the leaching and recovery of metals such as Pb, Zn and Ag, but it leaves a residue containing approximately 55% iron [13].

Corresponding author: romeroipn@hotmail.com

https://doi.org/10.2298/JMMB231219015J

Previous studies [14–16] and industrial processes [17] have shown that the pyrometallurgical treatment of jarosite can be divided into two functional steps. The first step of the treatment is carried out under oxidising conditions to decompose the material, releasing sulfates thermally and OH groups. During the second step, the molten oxide formed is reduced, and the volatile elements are removed to the gas phase. In this way, a clean slag and a liquid metal alloy are formed. The formation of the metal alloy during the reduction stage plays an important role due to its ability to collect various low-concentration metals from the material, such as Ag, As and Sb [15].

Pyrometallurgical treatment of jarosite–leaching residues has proven to be the most promising processing route, given its capability to generate clean slag and recover the most valuable metals [18, 19]. Nevertheless, developing and optimising the process necessitates a more detailed understanding of the processing possibilities and the effects of various parameters and variables.

In this study, high-temperature experiments were conducted on jarosite residue to explore the melting and reduction processes for the recovery of valuable metals and the transformation of jarosite residue into a clean slag product. A mixture of CaO-SiO_2 was introduced to the previously high–temperature roasted jarosite residue, along with the reducing agent CaSi, to facilitate melting and obtain a liquid slag. This process yielded metallic phases containing residual metals and eliminated noxious elements. The thermal decomposition of jarosite, as well as the analysis of the final slag and metallic phases, was performed using techniques such as differential scanning calorimetry (DSC), X-ray diffraction (XRD), scanning electron microscopy and energy dispersion spectrometer (SEM-EDS). Under Mexican environmental regulations [20], chemical stability tests were conducted on both the jarosite residue and the final slag.

2. Materials and methods

The jarosite residue utilised in this study was sourced from a domestic zinc smelter plant in Mexico and processed according to the ASTM C702/C702M-11 standard for collecting a representative sample [21]. The residue was heated for 8 h at 100 °C to eliminate humidity, followed by a chemical analysis using X-ray fluorescence.

Zhu et al. [22] reported that SO_4^{2-} constitutes the main S-bearing component of jarosite, requiring high temperature for S removal due to its elevated thermal stability. Therefore, after drying the jarosite residue at 100 °C, *in situ* high-temperature X-ray powder diffraction (Panalytical Empyrean diffractometer) was employed to estimate jarosite phase transformation, from room temperature to 950 °C.

The thermogravimetric analysis of the jarosite residue was conducted using thermogravimetry and differential scanning calorimetry (TG-DSC, Mettler Toledo Star 1). During the TG-DSC analysis, the sample underwent heating in an argon atmosphere at a rate of 15 °C/min from 25 °C to 1600 °C. Mass changes and thermal effects were recorded during the heating process, and TG-DSC curves were obtained. The compositions of the samples were determined by chemical analysis using atomic flame absorption. The morphology of the species and element distribution were analysed by scanning electron microscopy (SEM) together with an energy dispersive spectrometer (SEM–EDS, Jeol 6300). Additionally, X-ray Diffraction (XRD Bruker D8 Focus) analysis was conducted to identify crystalline compounds.

Fig. 1 illustrates the schematic flow diagram of the jarosite waste treatment process. The jarosite sample was initially prepared following ASTM C702/C702M-11 [21]. Subsequently, humidity was eliminated at 100 °C for 8 h. The roasting process occurred at 700 °C for 1 h in a laboratory muffle furnace. The roasted material was ground to a size of 74 μm (-200 mesh) and mixed with flux reagents (CaO and SiO_2) and a reducing agent (CaSi). The reduction step took place at 1400 °C for 1 h in an alumina crucible. Finally, the slag and metallic phases obtained in this process underwent characterisation

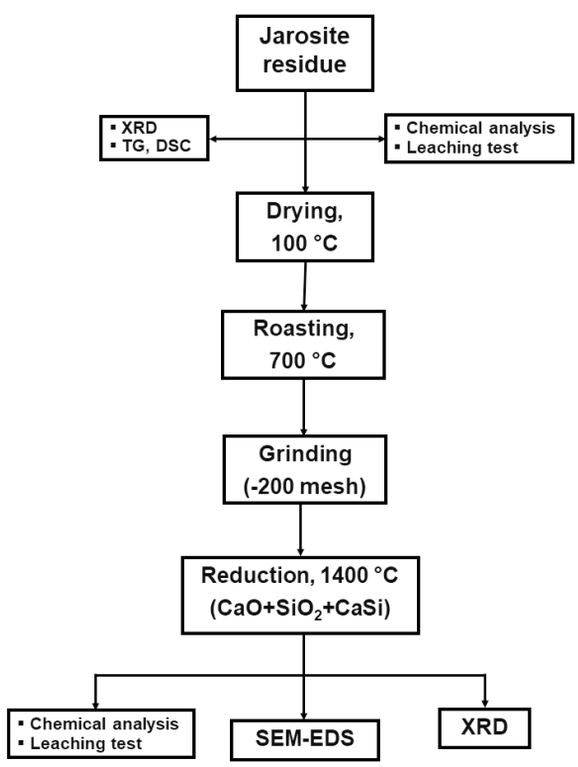

Figure 1. *Proposed flow diagram of the jarosite residue treatment process*

using XRD, chemical analysis and SEM-EDS. Moreover, the chemical stability of the final slag was estimated according to the Mexican environmental norm NOM-053-SEMARNAT-1993 [20].

A thermodynamic analysis, utilising FactSage v. 8.3 software [23] was conducted to assess the impact of the reducing agent (CaSi) quantity and $CaSO_4$ content on the equilibrium phases of the system. The software incorporates the initial mass, temperature, and system pressure to calculate the most stable species through Gibbs' free energy minimisation method.

The raw jarosite residue sample and the final slag obtained in the reduction process were crushed into a fine powder. The chemical stability of these materials was evaluated by a leaching technique, following Mexican environmental regulations [20]. It stipulates that 25 g of each material must be crushed below –200 mesh and put into contact with 500 cm^3 of an aqueous solution of acetic acid at pH = 2.88 ± 0.05 in a rotary system for 20 h at 30 ± 2 rpm. Then, the solid waste must be filtered through ashless filter paper (Whatman 542), and the liquid solution should be characterised by atomic absorption spectrometry.

3. Results and discussion

3.1. Chemical analysis results

Table 1 displays the elemental composition of the dried jarosite, while Fig. 2 shows the XRD pattern of the residue. The mineralogical species in the dried residue primarily included ammonium jarosite ($(NH_4)Fe_3(SO_4)_2(OH)_6$), gypsum ($CaSO_4{\cdot}2H_2O$) and a small amount of anhydrite ($CaSO_4$), blende (ZnS) and $ZnSO_4{\cdot}7H_2O$.

3.2. High-temperature XRD results

Fig. 3 depicts the phases obtained through the *in situ* high-temperature XRD technique. It is observed that small peaks of jarosite persist at 440 °C and were partially transformed into $Fe_2(SO_4)_3$ and Fe_2O_3, while it was completely decomposed into Fe_2O_3 and Fe_3O_4 at 650 °C. Increasing the temperature from 440 °C to 650 °C reduces the peak of $Fe_2(SO_4)_3$ and enhances the peaks of Fe_2O_3 and Fe_3O_4. The peak intensity of gypsum ($CaSO_4{\cdot}2H_2O$) decreased as temperature increased, and at 950 °C gypsum was completely dehydrated, yielding anhydrite ($CaSO_4$). The peaks of anglesite ($PbSO_4$) were observed only at high temperatures (650 °C and 950 °C). The *in situ* high-temperature XRD analysis showed that above 650 °C, nearly all jarosite compounds had decomposed.

3.3. TGA and DSC results

Fig. 4 illustrates the differential thermal patterns of jarosite ranging from 50 °C to 1600 °C. The jarosite residues underwent six stages during this heating process. In the initial stage (102 °C to 162 °C), the residues lost free and absorbed water. The second stage (163 °C to 416 °C) involved the removal of crystalline water from the jarosite. During the third stage (417 °C to 576 °C) jarosite decomposed into Fe_2O_3, SO_2 and H_2, iron hydroxide was transformed into Fe_2O_3, and anhydrite also appeared. Frost et al. [24] reported that the decomposition of jarosite is mainly carried out in two stages, the first one is between 280 °C and 450 °C with a substantial mass loss, while the second one releases S from sulfate in the form of SO_3 gas between 580 °C and 730 °C. This

Table 1. *Elemental chemical composition of the jarosite residue*

Element	O	Ca	Zn	Fe	S	Si	Na	Mg	Pb	As	Ag (ppm)	Others
wt%	48.35	12.65	4.19	11.05	17.20	1.05	0.93	0.18	3.57	0.23	144	0.6

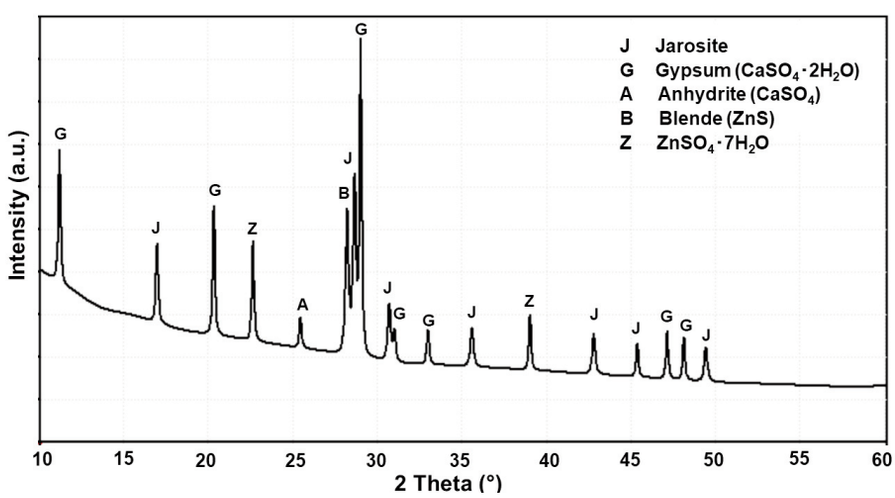

Figure 2. *XRD pattern of the jarosite residue*

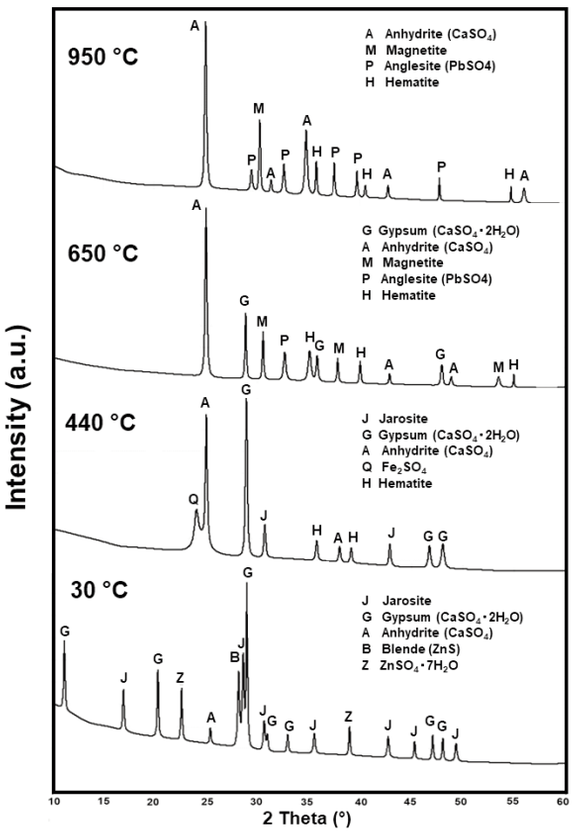

Figure 3. *XRD patterns of jarosite residues heated at different temperatures*

corresponds to the following reactions:

$$2\left[(NH_4)Fe_3(SO_4)_2(OH)_6\right] \rightarrow (NH_4)_2SO_4 + Fe_2(SO_4)_3 + 2Fe_2O_3 + 6H_2O \quad (1)$$

$$Fe_2(SO_4)_3 \rightarrow Fe_2O_3 + 3SO_3 \quad (2)$$

In the fourth stage (577 °C to 780 °C) the anhydrite remains, and the hematite is stabilised, in addition, some of the OH^- and sulfate groups are released by thermal decomposition. In the fifth stage (781 °C to 965 °C), anhydrite and hematite are preserved. In the sixth stage (966 °C to 1296 °C), the hematite remained stable. Graphically, the total weight loss amounted to 46.5%. These TGA results agree with those obtained by Linsong et al. [25].

Based on the XRD and TGA results, the roasting temperature selected for jarosite decomposition and sulfur removal in this study was 700 °C.

3.4. Reducing smelting results

The roasted jarosite mainly contains hematite and anhydrite. To achieve complete melting of this material and reduce metallic oxide species, a mixture of CaO and SiO_2 was used. The amounts of these oxides were estimated to obtain a silicate slag with a low melting temperature. Fig. 5 illustrates the CaO-SiO_2-Fe_2O_3 ternary phase diagram [26] which indicates that by using a mass ratio of CaO/SiO_2 = 48/52 = 0.92, a melting point of the slag at about 1300 °C can be obtained.

A thermodynamic analysis was carried out using the software FactSage v 8.3 [23] to estimate the impact of the quantity of the reducing agent CaSi and the presence of anhydrite ($CaSO_4$) in the roasted jarosite on the metallic phase obtained in equilibrium at 1400 °C. The amount (in g) of the initial species considered in this system is as follows:

$$2.1Fe_2O_3 + 1.872CaO + 2.0228SiO_2 + 0.1PbO + xCaSi + yCaSO_4 \quad (3)$$

It can be observed that the mass ratio CaO/SiO_2 was considered equal to 0.92, 'x' ranged from 0 to 2

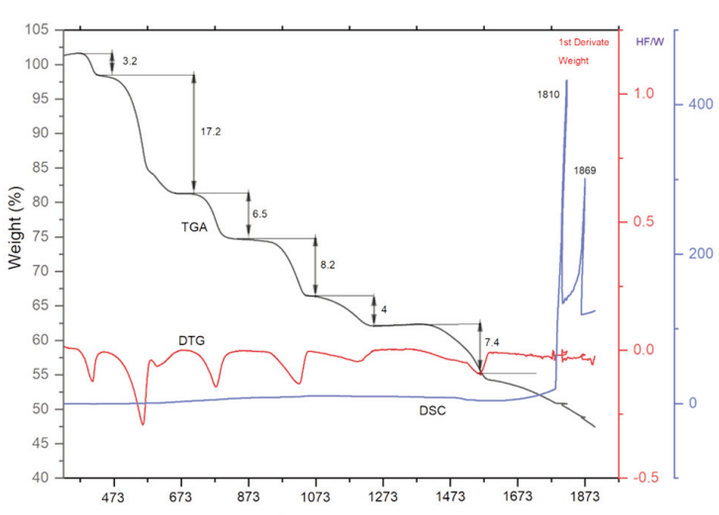

Figure 4. *Differential thermal patterns of jarosite TGA; Thermogravimetric analysis; DSC: Differential Scanning Calorimetry; DTG (Derived thermogravimetry)*

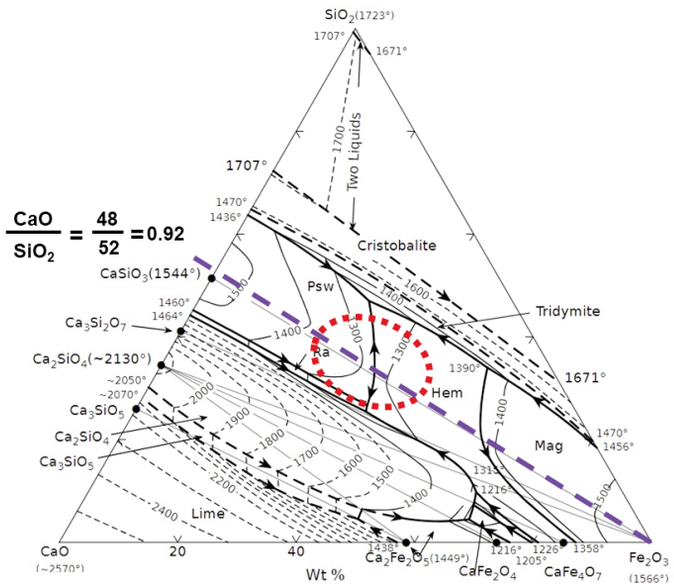

Figure 5. *CaO-SiO_2-Fe_2O_3 ternary phase diagram [26]*

g, and 'y' was 0 and 1 g. The results are illustrated in Fig. 6. Three main conclusions can be drawn from these results: (a) Two metallic phases can be obtained, liquid lead and a liquid Fe-Si alloy; (b) With low $CaSO_4$ content the first metallic phase formed is liquid lead, while with the increasing $CaSO_4$ content, an alloy of Fe-Si is initially obtained; (c) Increasing the amount of $CaSO_4$ requires an increased amount of the reducing agent (CaSi) to produce the metallic phases.

The above results were considered to programme a series of experiments with different amounts of reducing agents (CaSi). Table 2 presents the amount of CaSi used in the reducing trials. The tests were performed at 1400 °C by varying the content of CaSi as a reducing agent from 1 g to 3.5 g. The mass of roasted jarosite remained constant at 2.1 g, whereas the mass of the flux mixture (48%CaO, 52% SiO_2) was 3.9 g.

The results showed that Test number 1 did not produce any metallic phase due to the low amount of CaSi used. In Tests 2 and 3, a metallic phase, consisting of a Fe-Si alloy with no observable Pb-based alloy, was obtained. It is noteworthy that the Fe-Si alloy in Test 2 was magnetic, while that in Test 3 was non-magnetic due to a higher silicon content resulting from an increased amount of the reducing agent. Fig. 7 shows the SEM-EDS microanalysis of the Fe-Si phase from Test number 3, revealing the

Table 2. *Amount of CaSi used in the reducing trials*

Test Number	Mass of CaSi (g)
1	1
2	1.5
3	2
4	3
5	3.5

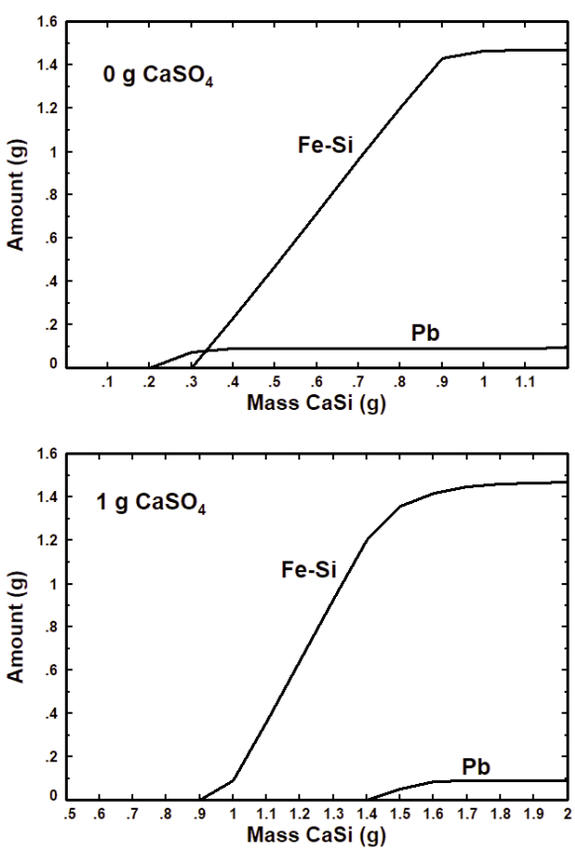

Figure 6. *Calculated effect of the reducing agent and $CaSO_4$ content on the metallic phases obtained at 1400 °C*

a)

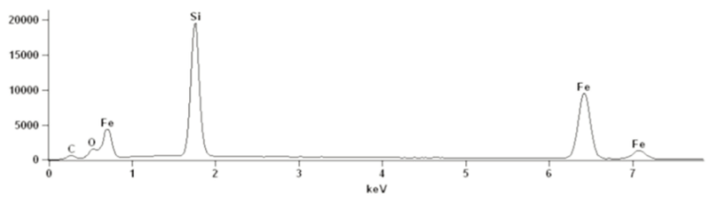

b)

Element Line	Weight %	Atom %
O K	7.99	18.15
Si K	34.14	44.18
Fe K	57.88	37.67
Total	100.00	100.00

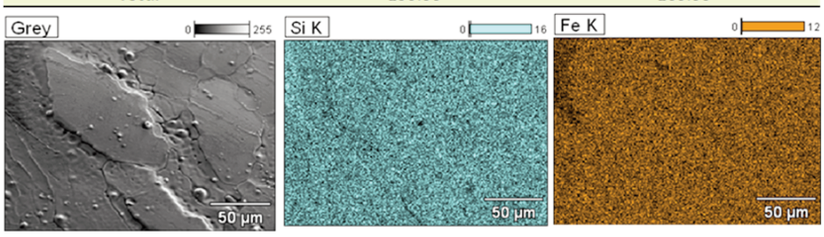

Figure 7. *(a) Microanalysis of non-magnetic Fe-Si in Test 3, (b) SEM micrograph and X-ray mapping images*

presence of Fe and Si, along with a small amount of oxygen.

Test 4 yielded a blend of metallic phases (Fe-Si and a Pb-based alloy) with non-magnetic traits. The slag produced constituted approximately 75% of the total mass employed. This slag underwent a leaching test. In Test number 5, featuring the highest CaSi mass, results mirrored those of Test number 4 concerning the Pb-based alloy. Nevertheless, there was an elevated Si content in the Fe-Si alloy.

Fig. 8 displays the micrograph of the metallic phases obtained in Test 4, along with microanalysis indicating the presence of elements Si, Fe, Cu, Ag, Pb, As, Sb and Zn in an Fe-Si matrix. It is observed that the main components of this phase are iron and silicon; however, Pb, along with valuable metals such as Ag and Zn, was also reduced in the process and collected in the Pb-rich metallic phase. To determine the distribution of elements in the metallic phases, Fig. 9 shows the SEM micrograph and corresponding X-ray elemental map obtained from SEM. This figure clearly shows that the round particles are composed of Pb, Zn and As, which are separated from a matrix composed of Fe and Si.

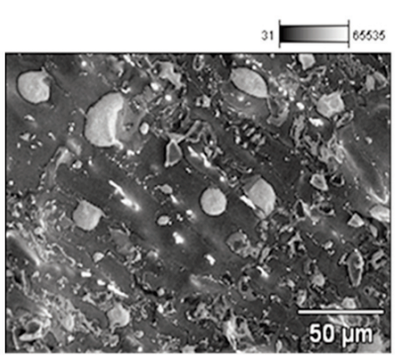

a)

b)

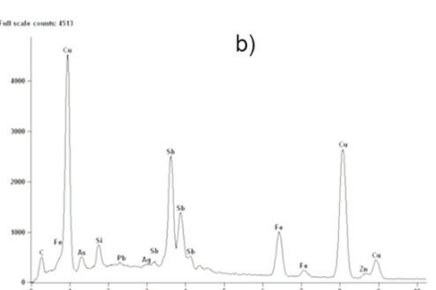

Element Line	Weight %	Weight % Error
Si K	47.07	+/- 0.23
Fe K	44.21	+/- 0.44
Cu K	1.51	+/- 0.16
Ag L	1.03	+/- 0.15
Pb M	3.88	+/- 0.23
As K	0.44	+/- 0.14
Sb K	0.99	+/- 0.19
Zn K	0.87	+/- 0.21
Total	100	

Figure 8. *(a) SEM micrograph of the metallic phases of Test 4, (b) Semiquantitative microanalysis*

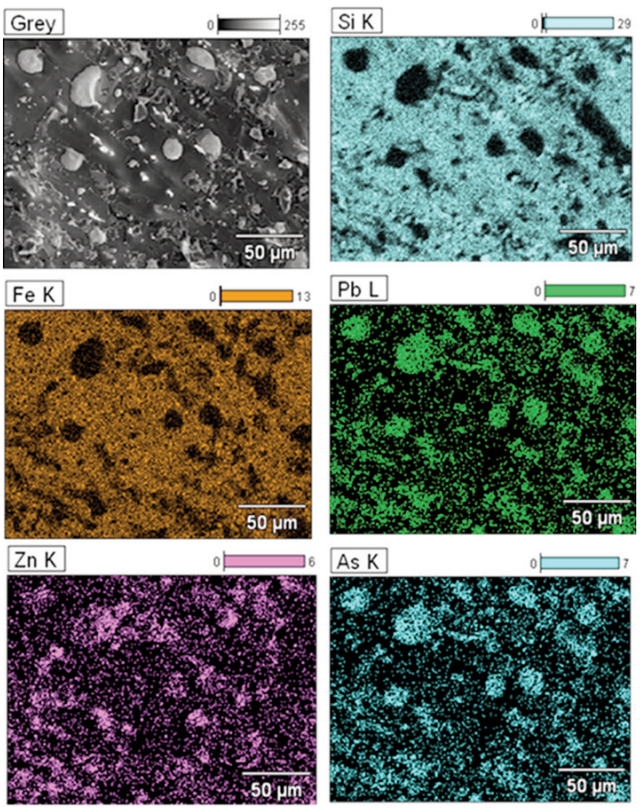

Figure 9. *X-ray mapping images of elements Si, Fe, Pb, Zn, and As for the metallic phases of Test number 4*

The composition of the mixture of the metallic phases was analysed for Zn, Pb and Ag. Table 3 reveals that Ag constituted 0.0091 wt.% (91ppm). Chemical analysis and SEM-EDS results confirm Ag accumulation, particularly in the Pb-based alloy. However, Zn content is lower than the jarosite residue value, suggesting significant Zn evaporation during the 1400 °C reduction process.

Table 3. *Global composition of the metallic phases*

	Zn	Pb	Ag	Fe+Si
wt.%	0.079	0.61	0.0091	Balance

The XRD pattern of the slag from Test number 4 is depicted in Fig. 10. This slag sample primarily comprises calcium silicates: rankinite ($Ca_3Si_2O_7$), wollastonite ($CaSiO_3$) and larnite (Ca_2SiO_4). These results show that Fe was completely reduced to the metallic Fe-Si alloy.

3.5. Leaching Results

Table 4 displays the results of the chemical analysis for the liquid solutions obtained after the leaching test in an acid solution for both the as-received jarosite residue and the final slag obtained after the reducing process in Test number 4. The final slag becomes environmentally friendly because the dissolved metals in the leaching test are lower than the recommended limits, especially for silver and lead.

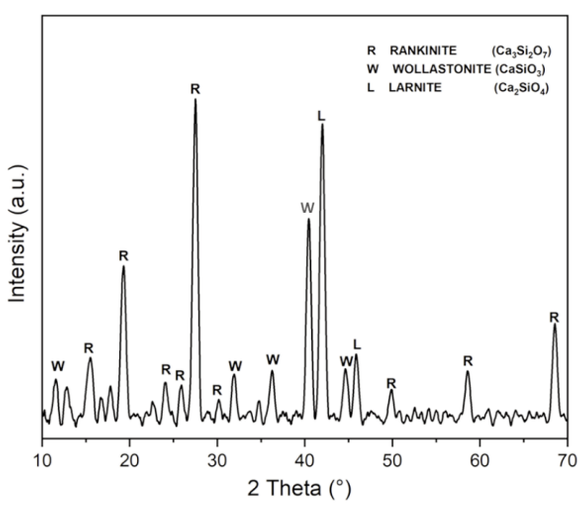

Figure 10. *XRD pattern of the final slag of test 4*

Table 4. *Leaching results of the jarosite residue and slag of Test number 4*

	Ag, mg/l	Pb, mg/l	Zn, mg/l
NOM-053-SEMARNAT-1993	5 max.	5 max.	–
Jarosite residue	7.4	16.7	11,300
Slag (test No. 4)	1.2	4.3	2,500

4. Conclusions

In the present work, a process for the treatment of jarosite waste was proposed in order to recover valuable metals and obtain an environmentally friendly final waste that could be used in other industries. In this process, the moisture was removed at 100 °C and roasted at 700 °C to decompose the jarosite and remove the sulfur. A reduction step was then carried out at 1400 °C by adding fluxes (CaO and SiO_2) and a reducing agent (CaSi). The conclusions from this work are as follows:

- The jarosite residues were decomposed into Fe_2O_3, Fe_3O_4 and $CaSO_4$ at a roasting temperature of 700 °C.
- A mixture of 48 wt% CaO and 52 wt% SiO_2 was used as flux for the roasted residue to obtain a completely liquid system. In addition to the fluxes, a CaSi-reducing agent was added to obtain a mixture of slag and metallic phases in the system.
- Two metallic phases were obtained, one of which consisted of Fe and Si, and the other was rich in Pb, which captured valuable and toxic metals, such as Ag, Zn, and As.
- The presence of $CaSO_4$ in the system affects the order and quantity in which the metal phases precipitate. A high $CaSO_4$ content requires the addition of a greater amount of reducing agent to form the metallic phases.
- The slag resulting from the reduction process complies with environmental regulations and could be used as a raw material in other industries.

Acknowledgments

The authors wish to thank the company Servicios Administrativos Peñoles, the National Council for Science and Technology (CONACYT), the National Polytechnic Institute (IPN), and the Researcher National System (SNI) for the support of this research.

Author's contributions

C. Jiménez-Lugos and J. López-Rodríguez performed the experiments. M. Flores-Favela characterised the samples using XRD. A. Hernández-Ramírez analysed the jarosite residue by TG and DSC. A. Romero-Serrano performed the data analyses and wrote the manuscript. A. Cruz-Ramírez performed the thermodynamic analysis. E. Colín-García analysis by SEM-EDS.

Data availability

The authors confirm that the data supporting the findings of this study are available within the article. Details on the thermodynamic simulation are available from the corresponding author upon request.

Conflict of interest

All authors declare that they have no conflicts of interest.

References

[1] J.E. Dutrizac, The effectiveness of jarosite species for precipitating sodium jarosite, Journal of Operation Management, 51 (1999) 30–32. https://doi.org/10.1007/ s11837-999-0168-6.

[2] M.K. Jha, V. Kumar, R.J. Singh, Review of hydrometallurgical recovery of zinc from industrial wastes, Resources Conservation and Recycling, 33 (2001) 1–22. https://doi.org/10.1016/ S0921-3449(00)00095-1.

[3] H. Ge, Z. Pan, F. Xie, D. Lu, W. Wang, S. Wu, Recovery of valuable metals by roasting of jarosite in cement kiln, Metals, 13 (2023) 250. https://doi.org/10.3390/ met13020250.

[4] M. Rämä, S. Nurmi, A. Jokilaakso, L. Klemettinen, P. Taskinen, J. Salminen, Thermal processing of jarosite leach residue for a safe disposable slag and valuable metals recovery, Metals, 8 (2018) 744. https://doi.org/10.3390/met8100744.

[5] N.G. Picazo-Rodríguez, F.R. Carrillo-Pedroza, A. Martínez Luévanos, M.J. Soria-Aguilar, I. Almaguer-Guzmán, Sº and jarosite behavior during recovery of values from the direct leaching residue of sphalerite using cyanide and glycine, Journal of Mining and Metallurgy, Section B-Metallurgy, 57 (3) (2021) 349–358. https://doi.org/10.2298/JMMB191221031P.

[6] J. Gisby, P. Taskinen, J. Pihlasalo, Z. Li, M. Tyrer, J. Pearce, K. Avarmaa, P. Björklund, H. Davies, M. Korpi, S. Martin, L. Pesonen, J. Robinson, MTDATA and the prediction of phase equilibria in oxide systems: 30 years of industrial collaboration, Metallurgical and Materials Transactions B, 48 (2017) 91–98. https://doi.org/10.1007/s11663-016-0811-x.

[7] Y.C. Li, X.B. Min, L.Y. Chai, M.Q. Shi, C.J. Tang, Q.W. Wang, Y.J. Liang, J. Lei, W.J. Liyang, Co-treatment of gypsum sludge and Pb/Zn smelting slag for the solidification of sludge containing arsenic and heavy metals, Journal of Environmental Management,181 (2016) 756–761. https://dx.doi.org/10.1016/j.jenvman.2016.07.031.

[8] A.A. González-Ibarra, F. Nava-Alonso, J.C. Fuentes-Aceituno, A. Uribe-Salas, Hydrothermal decomposition of industrial jarosite in alkaline media: The rate determining step of the process kinetics, Journal of Mining and Metallurgy, Section B-Metallurgy, 52 (2) B (2016) 135-142. https://doi.org/10.2298/JMMB150430016G.

[9] Y. Du, X. Tong, X. Xie, W. Zhang, H. Yang, Q. Song, Recovery of zinc and silver from zinc acid-leaching residues with reduction of their environmental impact using a novel water leaching-flotation process, Minerals, 11 (2021) 586. https://doi.org/10.3390/min11060586.

[10] D. Mombelli, C. Mapelli, C. Di Cecca, S. Barella, A. Gruttadauria, M. Ragona, M. Pisu, A. Viola, Characterization of cast iron and slag produced by jarosite sludges reduction via arc transferred plasma (ATP) reactor, Journal of Environmental Chemical Engineering, 6 (2018) 773–783.

https://doi.org/10.1016/j.jece.2018.01.006

[11] Y. Wang, H. Yang, W. Zhang, R. Song, B. Jiang, Study on recovery of lead, zinc, iron from jarosite residues and simultaneous sulfur fixation by direct reduction, Physicochemical Problems of Minereral Processing, 54 (2), (2018) 517-526. http://dx.doi.org/10.5277/ppmp1859.

[12] G.M. Jiang, P.E. Bing, Y.J. Liang, L.Y. Chai, Q.W. Wang, Q.Z. Li, H.U. Ming, Recovery of valuable metals from zinc leaching residue by sulfate roasting and water leaching, Transactions of Nonferrous Metals Society of China, 27 (2017) 1180–1187. https://doi.org/10.1016/S1003-6326(17)60138-9.

[13] J. Li, H. Ma, Zinc and lead recovery from jarosite residues produced in zinc hydrometallurgy by vacuum reduction and distillation, Green Processing and Synthesis, 7 (2018) 552–557. https://doi.org/10.1515/gps-2017-0079.

[14] N. Eftekhari, M. Kargar, Z. Rokhbakhsh, F. Zamin, N. Rastakhiz, Z. Manafi, A review on various aspects of jarosite and its utilization potentials, Annales de Chimie-Science des Matériaux, 44 (2020) 43–52. https://doi.org/10.18280/acsm.440106.

[15] H. Han, W. Sun, Y. Hu, B. Jia, H. Tang, Anglesite and silver recovery from jarosite residues through roasting and sulfidization-flotation in zinc hydrometallurgy, Journal of Hazardous Materials, 278 (2014) 49–54. https://doi.org/10.1016/j.jhazmat.2014.05.091.

[16] A.M. Ahamed, M.N. Pons, Q. Ricoux, S. Issa, F. Goettmann, F. Lapicque, New pathway for utilization of jarosite, an industrial waste of zinc hydrometallurgy, Minerals Engineering, 170 (2021) 107030. https://doi.org/10.1016/j.mineng.2021.107030.

[17] F. Zeng, W. Wei, M. Li, R. Huang, F. Yang, Y. Duan, Heavy metal contamination in rice-producing soils of Hunan province, China, and potential health risks, International Journal of Environmental Research and Public Health, 12 (2015) 15584–15593. https://doi.org/10.3390/ijerph121215005.

[18] S. Ju, Y. Zhang, Y. Zhang, P. Xue, Y. Wang, Clean hydrometallurgical route to recover zinc, silver, lead, copper, cadmium, and iron from hazardous jarosite residues produced during zinc hydrometallurgy, Journal of Hazardous Materials, 192 (2011) 554-558. https://doi.org/10.1016/j.jhazmat.2011.05.049.

[19] H. Ge, Z. Pan, F. Xie, D. Lu, W. Wang, S. Wu, Recovery of valuable metals by roasting of jarosite in cement kiln, Metals, 13 (2023) 250. https://doi.org/10.3390/ met13020250.

[20] Mexican Official Norms. NOM-053-ECOL (1993). http://www. Semarnat.gob.mx (accessed 21 September 2023).

[21] ASTM C702/C702M-18, Standard practice for reducing samples of aggregate to testing size. https://compass.astm.org/document/?contentCode=ASTM%7CC0702_C0702M-18%7Cen-US&proxycl=https%3A%2F%2Fsecure.astm.org&fromLogin=true (accessed 14 October 2023).

[22] D. Zhu, C. Yang, J. Pan, Z. Guo, S. Li, New pyrometallurgical route for separation and recovery of Fe, Zn, In, Journal of Cleaner Production 205 (2018) 781e788. https://doi.org/10.1016/j.jclepro.2018.09.152.

[23] C.W. Bale, E. Bélisle, P. Chartrand, S.A. Decterov, G. Eriksson, A.E. Gheribi, K. Hack, I.H. Jung, Y.B. Kang, J. Melançon, A.D. Pelton, S. Petersen, C. Robelin, J. Sangster, M-A Van Ende, FactSage thermochemical software and databases, 2010-2016, Calphad, 54 (2016) 35-53. https://doi.org/10.1016/j.calphad.2016.07.004.

[24] R. L. Frost, R. A. Wills, J. T. Kloprogge, W. Martens, Thermal decomposition, Journal of Thermal Analysis and Calorimetry, 84 (2) (2006) 489–496. https://doi.org/10.1007/s10973-005-6953-8.

[25] W. Linsong, Z. Peng, F. Yu, L. Sujun, Y. Yue, W. Li, S. Wei, Recovery of metals from jarosite of hydrometallurgy nickel production by thermal treatment leaching, Hydrometallurgy, 198 (2020) 105493. https://doi.org/10.1016/j.hydromet.2020.105493.

[26] A Muan, E. F. Osborn, Phase equilibria among oxides in steelmaking, Addison-Wesley Pub. Massachusetts, USA, 1965, 114.

PIROMETALURŠKA OBRADA JAROZITNOG OSTATKA SA MEŠAVINOM CaO, SiO_2 I CaSi

C. Jiménez-Lugos [a], M. Flores-Favela [b], A. Romero-Serrano [a,*], A. Hernández-Ramírez [a], J. López-Rodríguez [a], A. Cruz-Ramírez [a], E. Colin-García [a]

[a] Nacionalni politehnički institut, ESIKIE, Metalurgija i materijali, Meksiko Siti, Meksiko
[b] Administrativne usluge Penoles S.A de C.V. Prol. Comonfort Sur 2050, Col. L. Echeveria, Toreon, C.P. Coahuila, Meksiko

Apstrakt

U elektrolitičkoj proizvodnji cinka, gvožđe u rastvorima se uglavnom kontroliše taloženjem jarozita. Ovaj talog takođe sadrži vredne metale (Zn, Pb, Cu, Ag) i toksične elemente (Hg, Cd, As). Ova studija se bavi pirometalurškom obradom jarozitnog otpada u cilju izvlačenja metala i transformacije otpada u ekološki prihvatljivu šljaku. Prvo je uzorak zagrejan na 100 °C kako bi se uklonila vlaga, a zatim pržen na 700 °C da bi se termičkom dekompozicijom oslobodile neke OH^- i sulfatne grupe. Analiza ternarnog faznog dijagrama SiO_2-CaO-Fe_2O_3 pokazala je da se topitelj koji sadrži 48% CaO i 52% SiO_2 može koristiti za topljenje prženog jarozita na 1400 °C. Zatim su sprovedeni testovi sa redukcionim sredstvom (CaSi), što je rezultiralo smešom šljake i dve metalne faze, od kojih je jedna Fe-Si legura, a druga Pb-bogata faza koja sadrži vredni metal Ag. I metalne i šljakaste faze su okarakterisane hemijskom analizom, SEM-EDS i XRD metodama. Pored toga, jarozitni ostatak i finalna šljaka su podvrgnuti luženju vodenim rastvorom sirćetne kiseline kako bi se odredila njihova hemijska stabilnost. Dobijeni rezultati pokazuju da šljaka proizvedena nakon redukcije jarozitnog ostatka ispunjava ekološke specifikacije i mogla bi se koristiti kao sirovina u drugim industrijama.

Ključne reči: *Jarozit; Termička obrada; Dobijanje metala*